Text Supplement for ScholarWorks@UA collection

Seismic moment tensor catalog for crustal earthquakes in the Cook Inlet and Susitna region of southern Alaska

Vipul Silwal

Version 1: May 3, 2018

Attribution: If you use these files, please cite *Silwal et al.* (2018) and *Silwal* (2018).

Description of files

This collection is established for the submission of a manuscript (*Silwal et al.*, 2018).

Three catalogs of seismic moment tensors were generated using first-motion polarities, body waves, and surface waves. The best solution (M_0) was obtained through a grid-search in the moment tensor space using the 'cut-and-paste' (CAP) approach, which allows for different frequencies and time shifts on different portions of seismograms (*Silwal and Tape*, 2016; *Zhao and Helmberger*, 1994; *Zhu and Helmberger*, 1996; *Zhu and Ben-Zion*, 2013). The moment tensor approach was adapted and applied in *Silwal and Tape* (2016) for double couple moment tensors and in *Alvizuri and Tape* (2016) for full moment tensors. (*Silwal et al.*, 2018) updated the misfit function to take into account the polarity error. *Alvizuri et al.* (2018) applied the updated misfit function for estimation of full moment tensors and uncertainty.

A summary of files in the collection is listed in the following table:

figure	description	file name
Figure A1	Waveform fits for 9 events around Beluga	beluga_cap.pdf
Figure A2	Waveform fits for 22 events in Cook Inlet basin	cookinlet_cap.pdf
Figure A3	Waveform fits for 22 events in Susitna basin	susitna_cap.pdf
Figure B1	Moment tensor beachballs with input polarity for 9 events around Beluga	beluga_beach_cap.pdf
Figure B2	Moment tensor beachballs with input polarity for 22 events in Cook Inlet basin	cookinlet_beach_cap.pdf
Figure B3	Moment tensor beachballs with input polarity for 22 events in Susitna basin	susitna_beach_cap.pdf
–	text file catalog of moment tensors	sakmt_mech.txt
–	zipped set of text files of input parameters for moment tensor inversions	sakmt_weights.zip
–	this file: summary of collection	sakmt_scholarworks.pdf

Within each set of figures (A1, A2, A3, B1, B2, B3), the events are in chronological order by origin time.

Figures A1, A2, A3: Waveform fits

Waveform fits for 53 moment tensor inversions in south-central Alaska. Black are observed waveforms; red are synthetic waveforms computed using a frequency-wavenumber method (*Zhu and Rivera*, 2002) that assumes a (1D) layered model. The waveforms are fit separately within five time windows: P wave vertical component (PV), P wave radial component (PR), Rayleigh

wave vertical component (SurfV), Rayleigh wave horizontal component (SurfR), and Love wave transverse component (SurfT). At far left in each row is the station name, source-station distance in km, and station azimuth in degrees. Below each pair of waveforms are four numbers: the cross-correlation time shift between data and synthetics, the cross-correlation value, the percent of the misfit function represented by the waveform pair, and the amplitude ratio between waveforms, $\ln(A_{\mathrm{obs}}/A_{\mathrm{syn}})$, where A is the max value of the waveform within the time window.

The beachball represents the best solution M_0 (i.e., the global minimum of the misfit function). The beachball is plotted as a lower-hemisphere projection (standard seismological convention) of the moment tensor. The surrounding black dots denote the azimuthal location of the stations used, and the red crosses denote the lower hemisphere piercing points of the ray paths to the stations.

Here is a header for an example event in Figure A1: The four header lines are as follows:

1. `Event 20080126042942584 Model scak Depth 11`
   The event ID is derived from the origin time of 2008-01-26 04:29:42.584.
   The layered model used is `scak`, and the event depth is 11 km.

2. `FM 141 50 67 Mw 3.00 γ 0 δ 0 rms 3.345e-01 VR 88.8 pol_wt 0.30`
   The orientation of the moment tensor solution M_0 is strike 141°, dip 50°, rake 67°. The estimated magnitude is M_{w} 3.0. The source type of M_0 is expressed in terms of lune longitude $\gamma = 0°$ and lune latitude $\delta = 0°$. Since we are searching only in double couple space, γ and δ are zero for all solutions (see (*Alvizuri et al.*, 2018)). The waveform difference between data and synthetics is $RMS = 3.345e - 01$, and the variance reduction is $VR = 88.8\%$. These are based on a waveform difference measure that rewards using longer time windows and broader bandpass limits. This choice means that the VR cannot be directly compared with VR values reported in other studies. The factor `pol_wt = 0.30` determines the balance between polarity misfit and waveform misfit (i.e., 0.70 for this example). A value of 999.0 means that polarities are not used.

3. `Filter periods (seconds): Body:0.11-0.25. Surf:12.50-20.00 duration: 0.06/0.03 s`
   The body waves were filtered 0.11–0.25 s, the surface waves were filtered 12.50–20.00 s. In cases, where no surface wave are used the bandpass range is redundant.
   The source time function is a trapezoidal function whose duration is 0.06 s and whose rise time is half the duration. The duration is not an estimated source parameter but is set according to the target frequency of body waveforms (here 9 Hz).

4. `# norm L1 # Pwin 1.3 Swin 100 # N 19 Np 37 Ns 0`
   An L1 norm was used for the misfit function (e.g., *Silwal and Tape*, 2016). The (reference) P-window is 1.3 s long and the surface wave window is 100 s long. Again, these parameters are meaningful only if the body or surface wave components are used for inversion. From a total of 19 stations (N), 37 P wave windows (Np) and 0 surface wave windows (Ns) were used. In this example, surface wave bandpass and window length are not used.

The numbers below each station are

1. source–station epicentral distance, km

2. station azimuth, in degrees

3. time shift between picked P onset and synthetic P onset.

2

4. sign of the observed first-motion polarity , which is either 1 (up or compression) or -1 (down or dilatation). The number in parentheses is the predicted amplitude, which ranges between $\pm\sqrt{2}$; numbers close to zero indicate that the station is near a nodal surface of the radiation pattern for the assumed mechanism.

The four numbers below each pair of waveforms are

1. the cross-correlation time shift $\Delta T = T_{\mathrm{obs}} - T_{\mathrm{syn}}$ required for matching the synthetics $s(t)$ with the data $u(t)$. A positive time-shift means that the synthetics arrive earlier than the data and that the assumed velocity model is faster than the actual earth structure.

2. the maximum cross-correlation percentage between $u(t)$ and $s(t - \Delta T)$

3. the percentage of the total misfit

4. the amplitude ratio $\ln(A_{\mathrm{obs}}/A_{\mathrm{syn}})$ in each time window

Figures B1, B2, B3: Beachballs with polarities

Here is a header for an example event in Figure B1:
  The two header lines are as follows:

1. `Event 20080126042942584 Model 20080126042942584_scak_011`
   Same as the header line 1 for waveform fits plot.

2. `FM 141 50 67 Mw 3.00 γ 0 δ 0 rms 3.345e-01 VR 88.8 pol_wt 0.30`
   Same as the header line 2 for waveform fits plot.

   The dot ($\cdot$) at the station name outside mark the azimuthal location. The lower hemisphere piercing points are marked with cross (x). The upper hemisphere piercing points are marked with circle (o). For these stations, lower hemisphere piercing point is also marked in (x).

   Triangle is marked instead of (x) for stations with observed polarity specified in the weight file. The observed up polarity (compression) is marked with upward pointing triangle, whereas, the down polarity (dilation) is marked with downward pointing triangle. The triangles are colored green if observed and theoretical polarity matches for compressional quadrant, and, blue if observed and theoretical polarity matches for dialational quadrant. This makes it easier to visualize. The triangles are colored red if the observed polarity does not matches with the theoretical polarity of the moment tensor beachball.

Text file tables for moment tensor catalogs [sakmt_mech.txt]

Seismic moment tensor catalogs. Details can be found within the header lines, which also refer to *Kanamori* (1977); *Aki and Richards* (1980); *Silver and Jordan* (1982); *Minson et al.* (2007); *Tape and Tape* (2012, 2013, 2015).

Input text files used in the moment tensor inversion [sakmt_weights.zip]

We provide a text file for each of the 53 events in this study. These files show which stations and which time windows were used (or not) in each moment tensor inversion. It also shows the first-motion polarity observations that were used.

References

Aki, K., and P. G. Richards (1980), *Quantitative Seismology, Theory and Methods*, W. H. Freeman, San Francisco, Calif., USA.

Alvizuri, C., and C. Tape (2016), Full moment tensors for small events ($M_w < 3$) at Uturuncu volcano, Bolivia, *Geophys. J. Int.*, *206*, 1761–1783, doi:10.1093/gji/ggw247.

Alvizuri, C., V. Silwal, L. Krischer, and C. Tape (2018), Estimation of full moment tensors, including uncertainties, for nuclear explosions, volcanic events, and earthquakes, *J. Geophys. Res. Solid Earth* (in press), doi:10.1029/2017JB015325.

Kanamori, H. (1977), The energy release in great earthquakes, *J. Geophys. Res.*, *82*, 2981–2987.

Minson, S. E., D. S. Dreger, R. Bürgmann, H. Kanamori, and K. M. Larson (2007), Seismically and geodetically determined nondouble-couple source mechanisms from the 2000 Miyakejima volcanic earthquake swarm, *J. Geophys. Res.*, *112*, B10308, doi:10.1029/2006JB004847.

Silver, P. G., and T. H. Jordan (1982), Optimal estimation of scalar seismic moment, *Geophys. J. R. Astron. Soc.*, *70*, 755–787.

Silwal, V. (2018), Seismic moment tensor catalog for crustal earthquakes in the Cook Inlet and Susitna region of southern Alaska, ScholarWorks@UA: descriptor file, text file of catalog, figures with waveform fits, and input weight files.

Silwal, V., and C. Tape (2016), Seismic moment tensors and estimated uncertainties in southern Alaska, *J. Geophys. Res. Solid Earth*, *121*, 2772–2797, doi:10.1002/2015JB012588.

Silwal, V., C. Tape, and A. Lomax (2018), Crustal earthquakes in the Cook Inlet and Susitna region of southern Alaska, *Tectonophysics* (in prep).

Tape, W., and C. Tape (2012), A geometric setting for moment tensors, *Geophys. J. Int.*, *190*, 476–498, doi:10.1111/j.1365-246X.2012.05491.x.

Tape, W., and C. Tape (2013), The classical model for moment tensors, *Geophys. J. Int.*, *195*, 1701–1720, doi:10.1093/gji/ggt302.

Tape, W., and C. Tape (2015), A uniform parameterization of moment tensors, *Geophys. J. Int.*, *202*, 2074–2081, doi:10.1093/gji/ggv262.

Zhao, L.-S., and D. V. Helmberger (1994), Source estimation from broadband regional seismograms, *Bull. Seismol. Soc. Am.*, *84*(1), 91–104.

Zhu, L., and Y. Ben-Zion (2013), Parameterization of general seismic potency and moment tensors for source inversion of seismic waveform data, *Geophys. J. Int.*, *194*, 839–843, doi: 10.1093/gji/ggt137.

Zhu, L., and D. Helmberger (1996), Advancement in source estimation techniques using broadband regional seismograms, *Bull. Seismol. Soc. Am.*, *86*(5), 1634–1641.

Zhu, L., and L. A. Rivera (2002), A note on the dynamic and static displacements from a point source in multilayered media, *Geophys. J. Int.*, *148*, 619–627, doi:10.1046/j.1365-246X.2002.01610.x.

Event 20080126042942584 Model scak Depth 11
FM 141 50 67 Mw 3.00 γ 0 δ 0 rms 3.345e−01 VR 88.8 pol_wt 0.30
Filter periods (seconds): Body:0.11−0.25. Surf:12.50−20.00 duration: 0.06/0.03 s
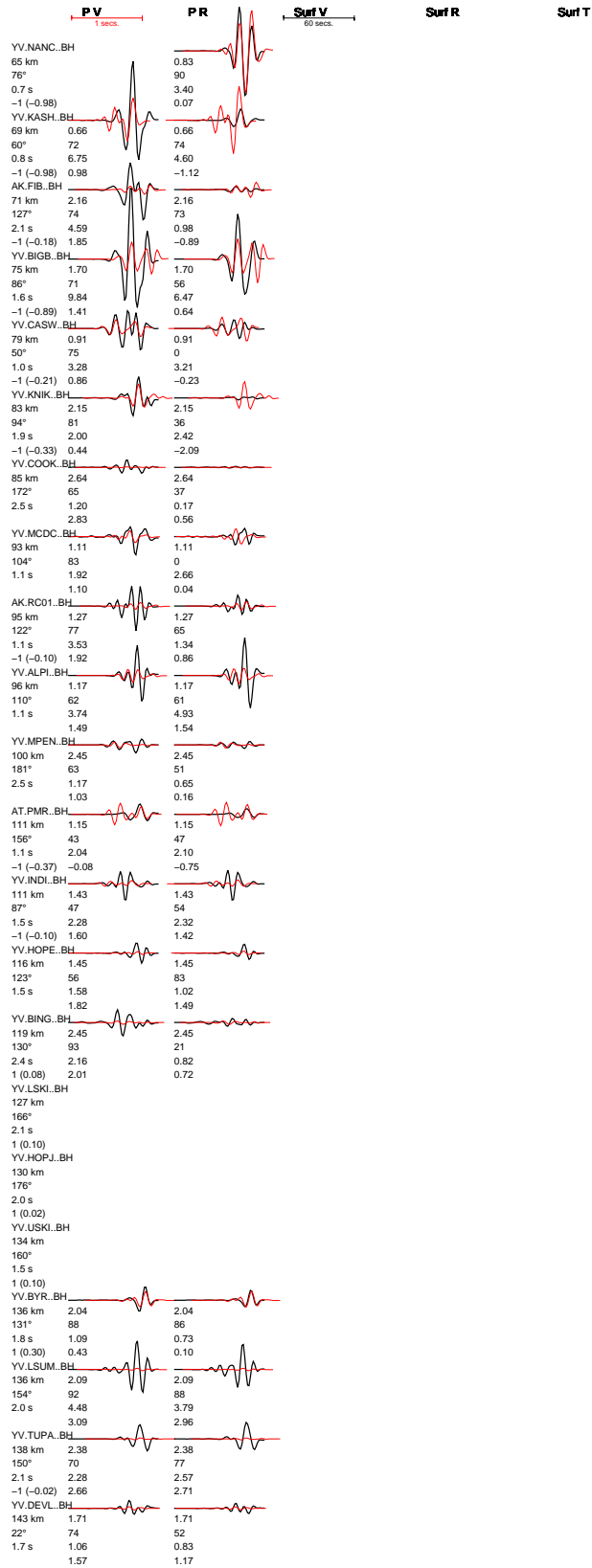# norm L1   # Pwin 1.3 Swin 100   # N 19 Np 37 Ns 0

P V	P R	Surf V	Surf R	Surf T
1 secs.		60 secs.		

YV.NANC..BH
65 km
76°   0.83
0.7 s   90
               3.40
−1 (−0.98)   0.07

YV.KASH..BH
69 km   0.66   0.66
60°   72   74
0.8 s   6.75   4.60
−1 (−0.98) 0.98 −1.12

AK.FIB..BH
71 km   2.16   2.16
127°   74   73
2.1 s   4.59   0.98
−1 (−0.18) 1.85 −0.89

YV.BIGB..BH
75 km   1.70   1.70
86°   71   56
1.6 s   9.84   6.47
−1 (−0.89) 1.41 0.64

YV.CASW..BH
79 km   0.91   0.91
50°   75   0
1.0 s   3.28   3.21
−1 (−0.21) 0.86 −0.23

YV.KNIK..BH
83 km   2.15   2.15
94°   81   36
1.9 s   2.00   2.42
−1 (−0.33) 0.44 −2.09

YV.COOK..BH
85 km   2.64   2.64
172°   65   37
2.5 s   1.20   0.17
         2.83   0.56

YV.MCDC..BH
93 km   1.11   1.11
104°   83   0
1.1 s   1.92   2.66
         1.10   0.04

AK.RC01..BH
95 km   1.27   1.27
122°   77   65
1.1 s   3.53   1.34
−1 (−0.10) 1.92 0.86

YV.ALPI..BH
96 km   1.17   1.17
110°   62   61
1.1 s   3.74   4.93
         1.49   1.54

YV.MPEN..BH
100 km   2.45   2.45
181°   63   51
2.5 s   1.17   0.65
         1.03   0.16

AT.PMR..BH
111 km   1.15   1.15
156°   43   47
1.1 s   2.04   2.10
−1 (−0.37) −0.08 −0.75

YV.INDI..BH
111 km   1.43   1.43
87°   47   54
1.5 s   2.28   2.32
−1 (−0.10) 1.60 1.42

YV.HOPE..BH
116 km   1.45   1.45
123°   56   83
1.5 s   1.58   1.02
         1.82   1.49

YV.BING..BH
119 km   2.45   2.45
130°   93   21
2.4 s   2.16   0.82
1 (0.08) 2.01   0.72

YV.LSKI..BH
127 km
166°
2.1 s
1 (0.10)

YV.HOPJ..BH
130 km
176°
2.0 s
1 (0.02)

YV.USKI..BH
134 km
160°
1.5 s
1 (0.10)

YV.BYR..BH
136 km   2.04   2.04
131°   88   86
1.8 s   1.09   0.73
1 (0.30) 0.43   0.10

YV.LSUM..BH
136 km   2.09   2.09
154°   92   88
2.0 s   4.48   3.79
         3.09   2.96

YV.TUPA..BH
138 km   2.38   2.38
150°   70   77
2.1 s   2.28   2.57
−1 (−0.02) 2.66 2.71

YV.DEVL..BH
143 km   1.71   1.71
22°   74   52
1.7 s   1.06   0.83
         1.57   1.17

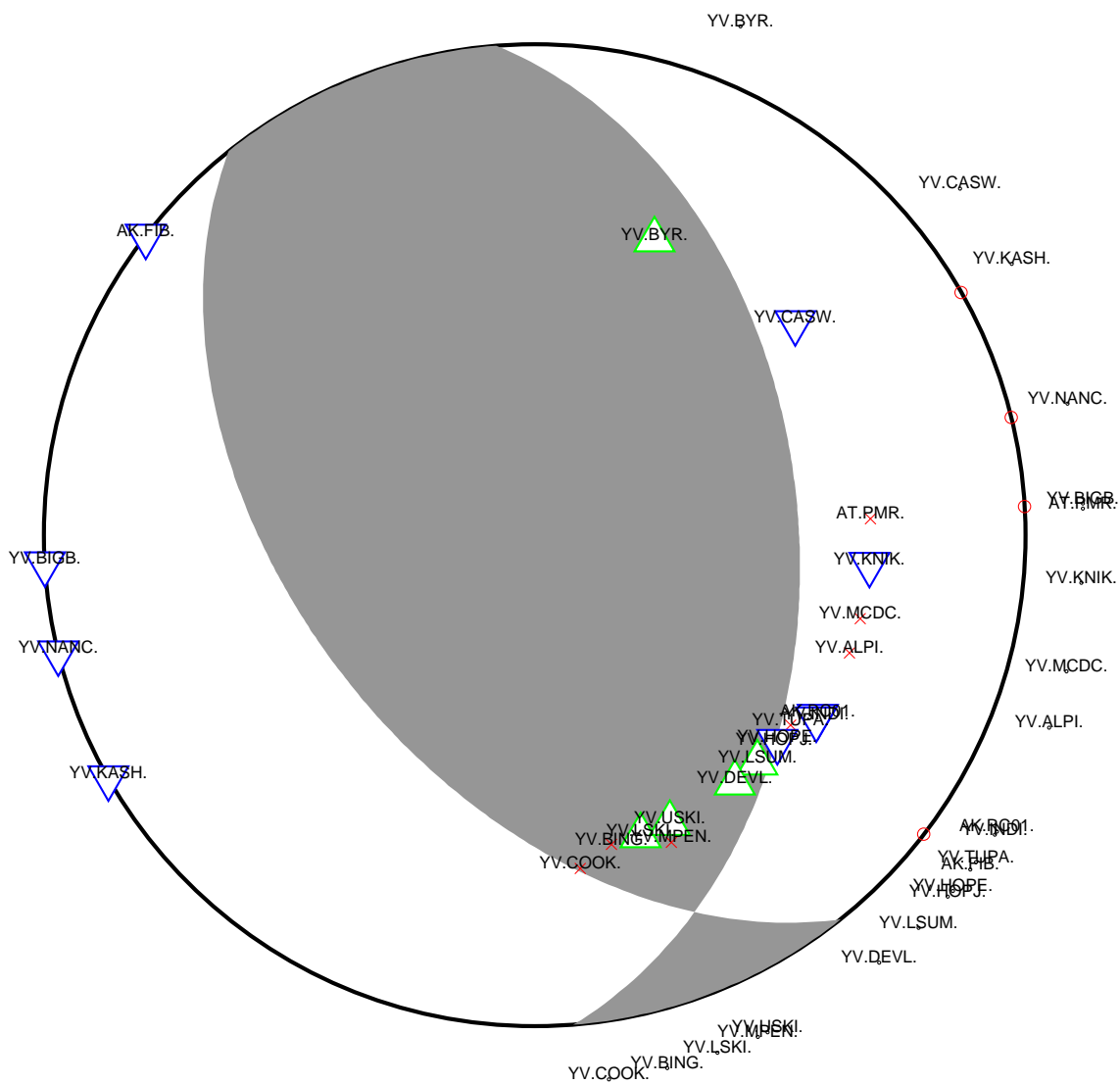Figure A1-1: Example from p. 1 of the set of 9 events in Figure A1.

Figure B1-1: Example from p. 1 of the set of 9 events in Figure B1.